A comparison of shot-encoding schemes for wave-equation migration

Jeff Godwin and Paul Sava, Center for Wave Phenomena, Colorado School of Mines*

SUMMARY

The seismic imaging industry is increasingly collecting data volumes with a substantial amount of redundancy through acquisition geometries including: wide-azimuth, rich-azimuth and full-azimuth. The increased redundancy improves image quality in areas with complex geology, but requires greater computational power to construct an image because of the additional data. One way to reduce the computational cost is to blend shot-records, together prior to imaging which reduces the number of migrations necessary for imaging. The downside to doing so is that blending introduces strong, non-physical, cross-talk noise into the final image. However, the crosstalk can be attenuated by carefully selecting a shot-encoding scheme. Many shot-encoding schemes have been proposed, but have not been directly compared to one another which makes it difficult to understand the relative advantages of the different schemes. We compare a few prominent shot-encoding schemes in a common theoretical framework and on a common dataset. Overall, we find that no single shot-encoding scheme is always better than others, and that decimated shot-record migration is advantageous over blended imaging.

INTRODUCTION

One idea to reduce the cost of imaging large datasets is to use multiple sources at once during imaging, which emulates simultaneous source acquisition. This process, known as blended imaging, combines multiple shot-gathers together prior to migration, which reduces the number of migrations that are needed to produce a final image (Morton, 1999; Liu, 1999; Romero et al., 2000; Soubaras, 2006; Zhang et al., 2007; Perrone and Sava, 2009; Berkhout et al., 2009). However, blending introduces strong, coherent noise referred to as crosstalk noise into the image.

Previous attempts to remove the crosstalk noise have focused on delaying the shot-records to shift the wavefields out of phase with one another. Some of the more prominent phase-encoding schemes include: plane-wave (Temme, 1984; Tieman, 1997; Stork, 1999; Liu, 1999; Duquet, 1999; Stoffa et al., 2006; Zhang et al., 2005; Liu et al., 2006; Shan and Biondi, 2008), random (Romero et al., 2000), harmonic (Zhang et al., 2007), plane-wave with dithering (Perrone and Sava, 2009), frequency dependent, sign-opposite (Sun, 1999) and modulated-shot migration (Soubaras, 2006).

However, these various shot-encoding schemes introduce different types of crosstalk noise into the stacked image. Thus, it is crucial to select the shot-encoding schemes that minimize the crosstalk noise during the imaging process. Subsequently, the two most important unresolved questions regarding blended imaging are: Does an optimal shot-encoding scheme exist that produces the best possible image at the lowest possible computational cost? If not, which of the already known shot-encoding schemes should be used?

The main goal of our work is to identify new shot-encoding schemes and to compare them against known shot-encoding schemes. We aim to demonstrate which shot-encoding schemes produce the best quality image at the lowest possible cost. To design new encoding schemes, we develop a theory of blended imaging that reframes the process of blending in terms of matrix operations. Also, we demonstrate how the same theory explains known shot-encoding schemes, including: plane-wave migration, modulated-shot migration and random time-delay encoding. We compare those schemes against decimated shot-record migration which is a convenient alternative to shot-encoding.

THEORY

The matrix theory of blended imaging revolves around the use of the encoding matrix $\mathbf{E}$ (Tieman, 1997; Soubaras, 2006). The encoding matrix is $N_s \times N_e$, where N_e is the number of blended experiments and N_s is the number of shots (wavefields) in the survey. Each column in the encoding matrix corresponds to a single blended experiment (realization), while each row acts as a weight for a particular source- or receiver-wavefield. To formally define the encoding matrix, we introduce the notation $E_{m,n}$, where the m index corresponds to the row (or shot index) and n corresponds to the column, or blended experiment index. The encoding matrix contains weights which may be fractional, positive or negative, and may even be complex-valued, but the physical meaning of the weights changes depending on their type. Additionally, it is possible to combine both amplitude and phase-shifts together, which can be represented mathematically as,

$$\mathbf{E}_{m,n} = A_{m,n} \exp(-j\phi_{m,n}), \tag{1}$$

where A is the amplitude weight for the mth shot-record for the nth blended experiment, $\phi_{m,n}$ is the corresponding phase-shift for the shot-record, and $j = \sqrt{-1}$. Amplitude only encodings are represented in equation 1 by letting $\phi_{m,n} = 0$ for all m and n. Phase-encodings are obtained when $A_{m,n} = 1$ for all m and n.

Matrix representation of blended imaging

The encoding matrix reduces the effective number of reconstructed wavefields that are used for imaging by projecting a $1 \times N_s$ vector containing all the source-

and receiver-wavefields for a survey, $\mathbf{W}_S$ or $\mathbf{W}_R$ respectively, onto the encoding matrix, thereby reducing the dimensionality of the wavefield vector as follows:

$$\mathbf{B} = \mathbf{WE}, then \begin{cases} \mathbf{B}_S &= \mathbf{W}_S\mathbf{E} \\ \mathbf{B}_R &= \mathbf{W}_R\mathbf{E} \end{cases} \tag{2}$$

where $\mathbf{B}$ is the blended wavefield vector for the source- or receiver-wavefields (i.e. $\mathbf{B}_S$ or $\mathbf{B}_R$). Because the migration operator is linear, we can perform the combination of the source- and receiver-data, the product of $\mathbf{WE}$, prior to wavefield reconstruction, thus reducing the necessary number of migrations from N_s to N_e. The final blended source image R_e is represented by

$$R_e = \mathbf{B}_S\mathbf{B}_R^H, \tag{3}$$

where H is the conjugate transpose. By substituting the expressions for $\mathbf{B}_S$ and $\mathbf{B}_R$ from equation 2 into equation 3, we obtain

$$R_e = \mathbf{W}_S\mathbf{E}\mathbf{E}^H\mathbf{W}_R^H. \tag{4}$$

We refer to the product $\mathbf{EE}^H$ as the crosstalk matrix $\mathbf{C}$, which is square and has dimensions of $N_s \times N_s$. Thus, equation 4 becomes,

$$R_e = R + X = \mathbf{W}_S\mathbf{C}\mathbf{W}_R^H, \tag{5}$$

where X represents the crosstalk noise added to the conventional image. The crosstalk matrix $\mathbf{C}$ is similar to the identity $\mathbf{I}$, but with additional off-diagonal terms. Thus, the $\mathbf{C}$ matrix represents the formation of the conventional seismic image (i.e. the diagonal terms) plus additional terms in the off-diagonals representing the pairing of wavefields that are not physically related to one another. The off-diagonal components of the $\mathbf{C}$ matrix are the crosstalk terms that we generate by using a certain encoding matrix $\mathbf{E}$ (Tieman, 1997; Soubaras, 2006). The crosstalk matrix allows us to determine the quality of the blended image prior to imaging.

SHOT-ENCODING SCHEMES

We compare the following shot-encoding schemes, which can be described using the previously discussed theory: Hartley amplitude encoding, modulated-shot migration, plane-wave migration and random time-delay encoding.

Hartley basis

A well-known orthonormal basis is the complex-valued discrete Fourier matrix (Strang, 1997; Oppenheim, 1999; Soubaras, 2006). A real-valued alternative to the Fourier basis is the Hartley basis (Strang, 1997; Tsitsas, 2010). The Hartley encoding matrix is defined as,

$$\mathbf{E}_{m,n} = cos\left(\frac{2\pi mn}{\wp}\right) + sin\left(\frac{2\pi mn}{\wp}\right), \tag{6}$$

where m is the shot-index, n is the encoding index, and $\wp$ is the periodization index (Soubaras, 2006). The presence of the addition between the sine and cosine introduces additional cross-terms into the crosstalk matrix because there are cross-terms between the sine and cosine during the matrix multiplication.

Modulated-shot migration (DFT)

Modulated-shot migration (DFT shot-encoding) is an encoding scheme that uses the discrete Fourier transform matrix as the encoding matrix (Soubaras, 2006). The encoding matrix is given as:

$$\mathbf{E}_{m,n} = \begin{cases} cos\,(Amn) - jsin\,(Amn)\,, & 0 \le n < N_e/2 \\ cos\,(Amn) + jsin\,(Amn)\,, & N_e \le n \le N_e \end{cases} \tag{7}$$

where m is the shot index, n is the encoding index, and A is $2\pi/\wp$ where $\wp$ is the periodization distance, which is typically N_s for the unitary DFT encoding matrix. Because we truncate the DFT matrix and we preferentially keep encodings corresponding to sinusoids with low angular frequencies, the DFT encoding matrix is equivalent to an optimal low-pass filter.

Plane-wave migration

For plane-wave migration, the encoding matrix is defined by the maximum time-delay and the number of encodings. The maximum time-delay determines the maximum wave-number in the blended image, and subsequently the crosstalk present in the final image (Tieman, 1997; Duquet, 1999; Liu, 1999; Stork, 1999; Zhang et al., 2005). To illustrate this consider the expression for the frequency-dependent encoding matrix for plane-wave migration:

$$\mathbf{E}_{m,n}(\omega) = exp(-j\omega\tau_{m,n}), \tag{8}$$

where $\tau_{m,n}$ is the time-delay in seconds, at the mth shot for the nth plane-wave encoding. The time-delay, $\tau_{m,n}$, is related to the shot position and the blended experiment by the relation,

$$\tau_{m,n} = \frac{(t_{max} - 2nt_{max}/N_e)m}{N_s} - \frac{t_{max} - 2nt_{max}/N_e}{2}, \tag{9}$$

where n is the nth encoding, m is the shot index,Δx is the shot-sampling interval, t_{max} is the maximum time-delay in seconds, and N_e is the number of blended experiments. Equation 9 requires $2t_{max}$ because plane-wave migration must create plane-waves with both positive and negative time-delays to ensure proper illumination throughout the image.

Random time-delay

Random time-delay encoding applies delays specified by a uniform distribution. The defining parameter for the uniform distribution is the maximum time-delay. Thus, the encoding matrix is given as:

$$\mathbf{E}_{m,n} = U(-t_{max}, t_{max}) \tag{10}$$

where U is a uniform probability distribution function with t_{max} the maximum time-delay for the shot-records. We can not formulate an analytic expression for the crosstalk matrix for random-time delay encoding. Instead, we can view the structure of the crosstalk matrix

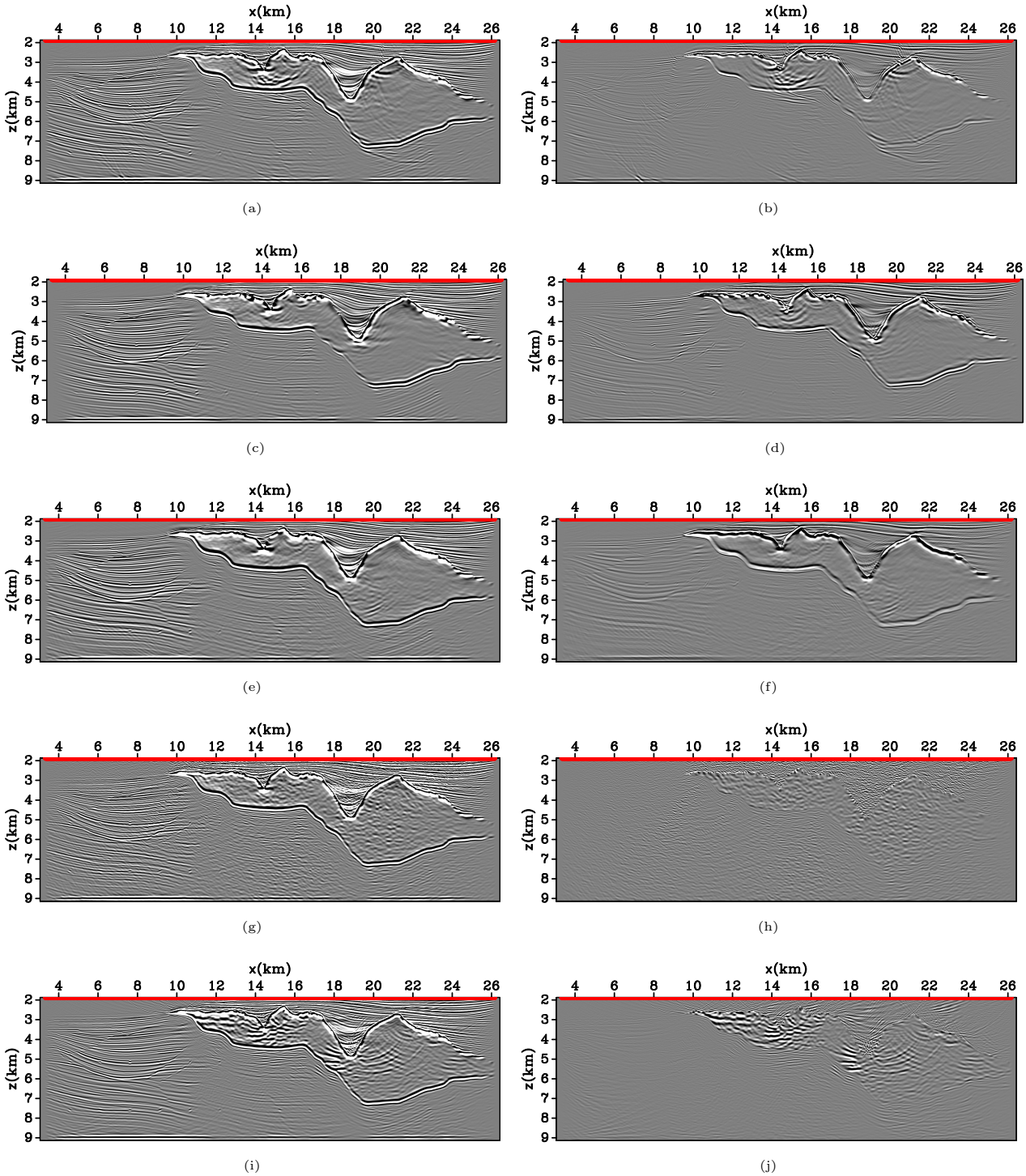

Figure 1: The stacked images (left) and difference images (right) for the following shot-encoding schemes (from top-bottom): Hartley, DFT (modulated-shot), plane-wave, random phase, and decimated shot-record migration. All encodings shown here use 50 encodings. The difference images are amplified 20×.

for one possible permutation of random time-delay encoding with the understanding that the crosstalk matrices for all similar encodings are more or less the same.

Decimated shot-record migration

As Stork (1999) and others have noted blended imaging is comparable to decimating our shot-records prior to imaging. Therefore, we compare different shot-encoding schemes compare against decimated shot-record migration (DSRM), because decimated shot-record migration has a few significant advantages over blended imaging: DSRM is easier to implement than shot-encoding because it does not require blending prior to imaging, and DSRM is less computationally expensive than blended imaging because each shot-record is migrated over a smaller aperture.

RESULTS

We compare the Hartley, DFT, Plane-wave, and random-time shot-encoding schemes for the original Sigsbee2A dataset, which is comprised of 500 shot-records. For each shot-encoding scheme, we construct the encoding matrix for 25, 50, 100, and 250 experiments. For Hartley and DFT encodings we use a periodization distance, $\wp = 250$, which is the optimal value for the Sigsbee dataset. For plane-wave and random-time delay encoding we use a maximum time-delay of 9.0 seconds, which is the theoretical maximum given by Stork (1999) for this dataset. Additionally, we compare the results of the encodings against the results obtained by using decimated shot-record migration using the same number of shot-records as encodings. In this way, the number of migrations for blended imaging and decimated shot-record migration are identical. We migrate the blended or decimated data using split-step downward continuation. Figure 1 shows the stacked images for all of the encoding schemes (including decimated SRM) and the difference images computed by subtracting the normalized blended image from the normalized image from conventional shot-record migration for 50 experiments. To make the comparison of difference images easier, we amplify them 20$\times$ and clip the difference images from all shot-encodings to the same scale. This ensures that changes in the difference images are directly comparable. For decimated shot-record migration, the difference image shows the artifacts introduced by aliasing.

As Figure 1 shows, the quality of the stacked image for blended imaging greatly depends on the choice of shot-encoding scheme and the number of encodings that we use for imaging. We note that Hartley, DFT, and plane-wave migration all show amplitude distortion of the reflectors because spatially close shots interfere strongly in the crosstalk matrix. Since these shots add up, the amplitudes of the reflectors are distorted overall. However, the best comparison of the shot-encoding schemes is to measure the energy in the difference images between the blended image and the conventional image using the l_2 norm of the difference image, Figure 2. This comparison shows that the best shot-encoding scheme varies with the number of encodings. For example, when using 25 encodings, random-time encoding produces the best quality image, whereas for 100 shot-encodings the best shot-encoding scheme is the Hartley amplitude encoding. However, decimated shot-record migration seemingly produces the best quality image at the lowest computational cost, even with the artifacts caused by spatial aliasing.

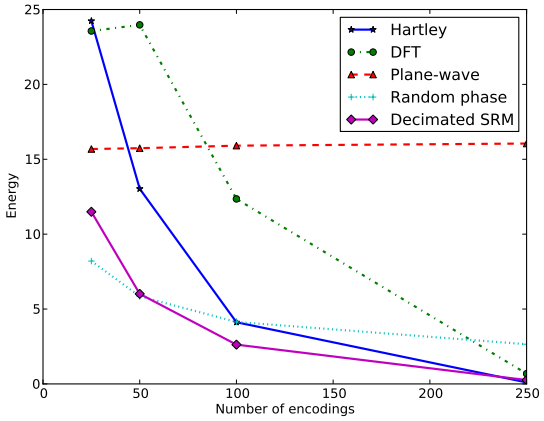

Figure 2: Plots of the energy (lower is better) in the difference image for the various shot-encoding schemes for a fixed number of experiments.

CONCLUSIONS

We develop a new class of shot-encoding schemes which modify the amplitudes of the shot-records prior to migration. We compare the results of the Hartley amplitude encoding with existing shot-encoding schemes including: modulated-shot migration, plane-wave migration, and random time-delay encoding, as well as with decimated shot record migration. The various shot-encodings produce images that have different crosstalk characteristics. We find that no one shot-encoding scheme excels over all the others in all circumstances. However, the best images at the lowest possible computational cost are obtained with decimated shot-record migration even in the presence of aliasing artifacts.

ACKNOWLEDGEMENTS

We want to thank the sponsors of the Center for Wave Phenomena for financial support on this project. Also, we want to thank Dave Hale and Francesco Perrone for their insights on various aspects of this project. We want to thank the contributors to the Madagascar software package available at http://www.reproduciblity.org .

REFERENCES

Berkhout, A., D. Verschuur, and G. Blacquiere, 2009, Seismic imaging with incoherent wavefields: SEG Technical Program Expanded Abstracts, 2894–2898.

Duquet, B., 1999, 3D plane wave migration of streamer data: SEG Technical Program Expanded Abstracts, **20**, 1033.

Liu, F., 1999, Plane wave source composition: An accurate phase encoding scheme for prestack migration: SEG Technical Program Expanded Abstracts, **21**, 1156.

Liu, F., D. W. Hanson, N. D. Whitmore, R. S. Day, and R. H. Stolt, 2006, Toward a unified analysis for source plane-wave migration: Geophysics, **71**, S129.

Morton, S. A., 1999, Fastershot-record depth migrations using phase encoding: SEG Technical Program Expanded Abstracts, **17**, 1131.

Oppenheim, A., 1999, Discrete-time signal processing, 2nd ed. ed.: Prentice Hall.

Perrone, F., and P. Sava, 2009, Comparison of shot encoding functions for reverse-time migration: SEG Technical Program Expanded Abstracts, 2980–2984.

Romero, L. A., D. C. Ghiglia, C. C. Ober, and S. A. Morton, 2000, Phase encoding of shot records in prestack migration: Geophysics, **65**, 426.

Shan, G., and B. Biondi, 2008, Plane-wave migration in tilted coordinates: Geophysics, **73**, S185.

Soubaras, R., 2006, Modulated-shot migration: SEG Technical Program Expanded Abstracts, **25**, 2430.

Stoffa, P. L., M. K. Sen, R. K. Seifoullaev, R. C. Pestana, and J. T. Fokkema, 2006, Plane-wave depth migration: Geophysics, **71**, S261.

Stork, C., 1999, How many p values do you want to migrate for delayed shot wave equation migration?: SEG Technical Program Expanded Abstracts, **23**, 1041.

Strang, G., 1997, Wavelets and filter banks, rev. ed. ed.: Wellesley-Cambridge Press.

Sun, P., 1999, Prestack migration of areal shot records with phase encoding: SEG Technical Program Expanded Abstracts, **21**, 1172.

Temme, P., 1984, A comparison of common-midpoint, single-shot, and plane-wave depth migration: Geophysics, **49**, 1896.

Tieman, H. J., 1997, Improving plane-wave decomposition and migration: Geophysics, **62**, 195.

Tsitsas, N. L., 2010, On block matrices associated with discrete trigonometric transforms and arising in wave propagation theory: Journal of Computational Mathematics.

Zhang, Y., J. Sun, and S. Gray, 2007, Reverse-time migration: Amplitude and implementation issues: SEG Technical Program Expanded Abstracts, **26**, 2145.

Zhang, Y., J. Sun, C. Notfors, S. H. Gray, L. Chernis, and J. Young, 2005, Delayed-shot 3D depth migration: Geophysics, **70**, E21.